2014 American Control Conference (ACC)
June 4-6, 2014. Portland, Oregon, USA

Adaptive Stabilization and Command Following Using a Prandtl-Ishlinskii/NARMAX Controller

Mohammad Al Janaideh and Dennis S. Bernstein

***Abstract*— We investigate a NARMAX controller structure involving hysteretic nonlinearities. A weighted combination of backlash nonlinearities constitutes a Prandtl-Ishlinskii hysteresis model. The rationale for using a Prandtl-Ishlinskii NARMAX (PIN) controller is due to the fact that the describing function of a backlash nonlinearity has both gain and phase shift. By combining backlash nonlinearities into a NARMAX control law it is reasonable to expect that arbitrary gain and phase shift can be attained by adaptively updated controller coefficients.**

I. Introduction

Hysteresis arises naturally in a wide variety of phenomena, from biological to engineering systems [1][2]. Hysteresis is beneficial when the objective is energy dissipation, but may degrade performance when hysteretic actuators are used for precision motion control [3][4]. As a feedback control element, hysteretic control laws are often used intentionally. For example, thermostats are typically employed to avoid chattering, which can damage on-off actuators [5]. Hysteretic actuators also help avoid chattering due to noise in switching controllers [5].

In the present paper we investigate a NARMAX controller structure involving hysteretic nonlinearities. NARMAX controllers are ARMAX control laws with nonlinear functions of the past inputs and outputs [6][7]. Although NARMAX control laws are nonlinear, they are linear in the controller parameters, which facilitates their use in control and identification. In the present paper we consider NARMAX control laws with backlash nonlinearities. A weighted combination of backlash nonlinearities constitutes a Prandtl-Ishlinskii hysteresis model [13][14]. Consequently, the control law we consider is a Prandtl-Ishlinskii NARMAX (PIN) controller.

The rationale for using the PIN controller is due to the fact that the describing function of a backlash nonlinearity has both gain and phase shift. By combining backlash nonlinearities into a NARMAX control law it is reasonable to expect that arbitrary gain and phase shift can be attained by suitable choice of controller coefficients. The PIN control law would then be applicable to command-following problem involving harmonic exogenous signals. Unfortunately, no guidelines are known for tuning a PIN control law. Consequently, in the present paper we adopt an adaptive control approach, where we let the adaptation mechanism tune the coefficients of the PIN control based on the closed-loop performance. For this purpose we use retrospective cost adaptive control (RCAC), which uses measurements of past performance to update the controller coefficients [9].

The objective of this paper is to numerically investigate the feasibility of using the adaptively tuned PIN control law for command-following problem involving harmonic exogenous signals. We thus consider a collection of examples that are chosen to illustrate the performance of the combined RCAC/PIN controller. We are particularly interested in examining the speed of adaptation, the transient and steady-state performance, the ability of RCAC/PIN to stabilize unstable systems, and the performance of RCAC/PIN in the presence of nonminimum-phase zeros.

The contents of the paper are as follows. In Section II, we formulate the problem. Section III presents the Prandtl-Ishlinskii NARMAX (PIN) controller. Section IV presents the simulation results. Section V concludes the paper.

II. Problem Formulation

In this section we consider

$$x(k+1) = Ax(k) + B\mathcal{N}(u(k)), \tag{1}$$

$$v(k) = \mathcal{N}(u(k)), \tag{2}$$

$$y(k) = Cx(k), \tag{3}$$

$$z(k) = r(k) - y(k), \tag{4}$$

where $\mathcal{N} : \mathbb{R} \to \mathbb{R}$ and the linear plant G. The goal is to develop an adaptive output feedback controller that minimizes the command-following error z with minimal modeling information about the plant G, and input nonlinearity $\mathcal{N}$. We assume that measurements of $y(k)$ are available for feedback; however, measurements of $v(k) = \mathcal{N}(u(k))$ are not available.

III. A Describing-Function for the Prandtl-Ishlinskii Hysteresis

In this section a describing function for the Prandtl-Ishlinskii Hysteresis is presented. Let $w(k) = \mathrm{Re}\{A_w e^{\jmath\Omega k}\}$, where A_w is a complex number. For $i = 1, \ldots, n$, let

$$u_i(k) = \Phi_{d_i}[w](k). \tag{5}$$

For $|A_w| > d_i$,

$$u_i(k) \cong \mathrm{Re}\big\{|A_w||F_i(|A_w|)|e^{\jmath(\Omega k + \angle F_i(|A_w|))}\big\}, \tag{6}$$

where the amplitude $|F_i(|A_w|)|$ and phase $\angle F_i(|A_w|)$ of the describing function of the backlash operator are given by [11]

$$|F_i(|A_w|)| = \frac{1}{|A_w|}\sqrt{{a_i}^2 + {b_i}^2}, \tag{7}$$

M. Al Janaideh is with the Department of Mechatronics Engineering, The University of Jordan, Amman 11942, Jordan. D. S. Bernstein is with the Department of Aerospace Engineering, The University of Michigan, Ann Arbor, MI 48109.

978-1-4799-3271-9/$31.00 ©2014 AACC

$$\angle F_i(|A_w|) = \tan^{-1}\frac{a_i}{b_i}, \tag{8}$$

where

$$a_i \triangleq \frac{2d_i}{\pi}\left(\eta_{\rho i} - 1\right), \tag{9}$$

$$b_i \triangleq \frac{|A_w|}{\pi}\left(\frac{\pi}{2} - \sin^{-1}\eta_{\rho i} - \eta_{\rho i}\sqrt{1-\eta_{\rho i}^2}\ \right), \tag{10}$$

where

$$\eta_{\rho i} \triangleq \frac{2d_i}{|A_w|} - 1.$$

The describing function of the Prandtl-Ishlinskii hysteresis model is given approximately by

$$H(\Omega, |A_w|) \triangleq \sum_{i=1}^{n} \kappa_i \mathrm{Re}\big\{|F_i(|A_w|)|e^{\jmath(\angle F_i(|A_w|))}\big\}. \tag{11}$$

Then, the output of the Prandtl-Ishlinskii hysteresis model is thus given approximately by

$$u(k) \triangleq \sum_{i=1}^{n} \kappa_i \mathrm{Re}\big\{A_w|F_i(|A_w|)|e^{\jmath(\Omega k + \angle F_i(|A_w|))}\big\}. \tag{12}$$

The describing function of the Prandtl-Ishlinskii hysteresis has both gain and phase shift. By combining Prandtl-Ishlinskii nonlinearity into a NARMAX control law it is reasonable to expect that arbitrary gain and phase shift can be attained by suitable choice of controller coefficients. The PIN control law would then be applicable to command-following problem involving harmonic exogenous signals.

IV. Prandtl-Ishlinskii NARMAX (PIN) controller

In this section we present the Prandtl-Ishlinskii NARMAX (PIN) controller. Consider the controller of order n_c given by

$$u(k) = \kappa_1 u(k-1) + \sum_{i=2}^{n_\mathrm{c}} \kappa_i(k)\Phi_{r_i}[z](k-1), \tag{13}$$

where, for all $i = 1, \ldots, n_\mathrm{c}$ and $\kappa_i(k) \in \mathbb{R}$ and

$$\Phi_{r_i}[z](k-1) = \tag{14}$$
$$\max(z(k-1) - d_i, \min(z(k-1) - d_i, \xi_i(k-2))),$$

where

$$\xi_i(k-2) = \Phi_{r_i}[z](k-2).$$

The control (13) can be expressed as

$$u(k) = \theta(k)\phi(k-1),$$

where

$$\theta(k) \triangleq \big[\kappa_1(k) \cdots \kappa_{n_\mathrm{c}}(k)\big]$$

is the controller gain matrix $\theta(k) \in \mathbb{R}^{n_\mathrm{c}}$, and the regressor vector $\phi(k) \in \mathbb{R}^{n_\mathrm{c}}$ is given by

$$\phi(k-1) \triangleq [u(k-1) \quad \Phi_{r_2}[z](k-1) \quad \cdots \quad \Phi_{r_{nc}}[z](k-1)]^\mathrm{T}.$$

A. Retrospective Cost Adaptive Control

We use retrospective cost adaptive control (RCAC), which uses measurements of past performance to update the controller coefficients of the Prandtl-Ishlinskii NARMAX (PIN) controller. For $i \geq 1$, define the Markov parameter

$$H_i \triangleq CA^{i-1}B.$$

For example, $H_1 = CB$ and $H_2 = CAB$. Let ℓ be a positive integer. Then, for all $k \geq \ell$,

$$x(k) = A^\ell x(k-\ell) + \sum_{i=1}^{\ell} A^{i-1}B\mathcal{N}(\mathrm{sat}(u(k-i))), \tag{15}$$

and thus

$$z(k) = CA^\ell x(k-\ell) - r(k) + \bar{H}\bar{U}(k-1), \tag{16}$$

where

$$\bar{H} \triangleq \begin{bmatrix} H_1 & \cdots & H_\ell \end{bmatrix} \in \mathbb{R}^{1\times\ell}$$

and

$$\bar{U}(k-1) \triangleq \begin{bmatrix} \mathcal{N}\big(\mathrm{sat}(u(k-1))\big) \\ \vdots \\ \mathcal{N}\big(\mathrm{sat}(u(k-\ell))\big) \end{bmatrix}.$$

Next, we rearrange the columns of $\bar{H}$ and the components of $\bar{U}(k-1)$ and partition the resulting matrix and vector so that

$$\bar{H}\bar{U}(k-1) = \mathcal{H}'U'(k-1) + \mathcal{H}U(k-1), \tag{17}$$

where $\mathcal{H}' \in \mathbb{R}^{1\times(\ell - l_U)}$, $\mathcal{H} \in \mathbb{R}^{1\times l_U}$, $U'(k-1) \in \mathbb{R}^{\ell - l_U}$, and $U(k-1) \in \mathbb{R}^{l_U}$. Then, we can rewrite (16) as

$$z(k) = \mathcal{S}(k) + \mathcal{H}U(k-1), \tag{18}$$

where

$$\mathcal{S}(k) \triangleq CA^\ell x(k-\ell) - r(k) + \mathcal{H}'U'(k-1). \tag{19}$$

Next, for $j = 1, \ldots, s$, we rewrite (18) with a delay of k_j time steps, where $0 \leq k_1 \leq k_2 \leq \cdots \leq k_s$, in the form

$$z(k-k_j) = \mathcal{S}_j(k-k_j) + \mathcal{H}_j U_j(k-k_j-1), \tag{20}$$

where (19) becomes

$$\mathcal{S}_j(k-k_j) \triangleq E_1 A^\ell x(k-k_j-\ell) + \mathcal{H}_j' U_j'(k-k_j-1)$$

and (17) becomes

$$\bar{H}\bar{U}(k-k_j-1) = \mathcal{H}_j' U_j'(k-k_j-1) + \mathcal{H}_j U_j(k-k_j-1),$$

where $\mathcal{H}_j' \in \mathbb{R}^{1\times(\ell - l_{U_j})}$, $\mathcal{H}_j \in \mathbb{R}^{1\times l_{U_j}}$, $U_j'(k-k_j-1) \in \mathbb{R}^{\ell - l_{U_j}}$, and $U_j(k-k_j-1) \in \mathbb{R}^{l_{U_j}}$. Now, by stacking $z(k-k_1), \ldots, z(k-k_s)$, we define the *extended performance*

$$Z(k) \triangleq \begin{bmatrix} z(k-k_1) \\ \vdots \\ z(k-k_s) \end{bmatrix} \in \mathbb{R}^s. \tag{21}$$

Therefore,

$$Z(k) \triangleq \tilde{\mathcal{S}}(k) + \tilde{\mathcal{H}}\tilde{U}(k-1), \tag{22}$$

where

$$\tilde{\mathcal{S}}(k) \triangleq \begin{bmatrix} \mathcal{S}_1(k-k_1) \\ \vdots \\ \mathcal{S}_s(k-k_s) \end{bmatrix} \in \mathbb{R}^s,$$

$\tilde{U}(k-1)$ has the form

$$\tilde{U}(k-1) \triangleq \begin{bmatrix} \mathcal{N}\big(\mathrm{sat}(u(k-q_1))\big) \\ \vdots \\ \mathcal{N}\big(\mathrm{sat}(u(k-q_{l_{\tilde{U}}}))\big) \end{bmatrix} \in \mathbb{R}^{l_{\tilde{U}}},$$

where, for $i = 1, \ldots, l_{\tilde{U}}$, $k_1 \le q_i \le k_s + \ell$, and $\tilde{\mathcal{H}} \in \mathbb{R}^{s \times l_{\tilde{U}}}$ is constructed according to the structure of $\tilde{U}(k-1)$. The vector $\tilde{U}(k-1)$ is formed by stacking $U_1(k-k_1-1), \ldots, U_s(k-k_s-1)$ and removing copies of repeated components. Next, for $j = 1, \ldots, s$, we define the *retrospective performance*

$$\hat{z}_j(k-k_j) \triangleq \mathcal{S}_j(k-k_j) + \mathcal{H}_j \hat{U}_j(k-k_j-1), \tag{23}$$

where the past controls $U_j(k-k_j-1)$ in (20) are replaced by the retrospective controls $\hat{U}_j(k-k_j-1)$. In analogy with (21), the *extended retrospective performance* for (23) is defined as

$$\hat{Z}(k) \triangleq \begin{bmatrix} \hat{z}_1(k-k_1) \\ \vdots \\ \hat{z}_s(k-k_s) \end{bmatrix} \in \mathbb{R}^s$$

and thus is given by

$$\hat{Z}(k) = \tilde{\mathcal{S}}(k) + \tilde{\mathcal{H}}\hat{\tilde{U}}(k-1), \tag{24}$$

where the components of $\hat{\tilde{U}}(k-1) \in \mathbb{R}^{l_{\tilde{U}}}$ are the components of $\hat{U}_1(k-k_1-1), \ldots, \hat{U}_s(k-k_s-1)$ ordered in the same way as the components of $\tilde{U}(k-1)$. Subtracting (22) from (24) yields

$$\hat{Z}(k) = Z(k) - \tilde{\mathcal{H}}\tilde{U}(k-1) + \tilde{\mathcal{H}}\hat{\tilde{U}}(k-1). \tag{25}$$

Finally, we define the *retrospective cost function*

$$J(\hat{\tilde{U}}(k-1), k) \triangleq \hat{Z}^{\mathrm{T}}(k) R(k) \hat{Z}(k), \tag{26}$$

where $R(k) \in \mathbb{R}^{s \times s}$ is a positive-definite performance weighting. The goal is to determine refined controls $\hat{\tilde{U}}(k-1)$ that would have provided better performance than the controls $U(k)$ that were applied to the system. The refined control values $\hat{\tilde{U}}(k-1)$ are subsequently used to update the controller.   Next, to ensure that (26) has a global minimizer, we consider the regularized cost

$$\bar{J}(\hat{\tilde{U}}(k-1), k) \triangleq \hat{Z}^{\mathrm{T}}(k) R(k) \hat{Z}(k) + \eta(k) \hat{\tilde{U}}^{\mathrm{T}}(k-1)\hat{\tilde{U}}(k-1), \tag{27}$$

where $\eta(k) \ge 0$. Substituting (25) into (27) yields

$$\bar{J}(\hat{\tilde{U}}(k-1), k) = \hat{\tilde{U}}(k-1)^{\mathrm{T}} \mathcal{A}(k) \hat{\tilde{U}}(k-1) + \mathcal{B}(k)\hat{\tilde{U}}(k-1) + \mathcal{C}(k), \tag{28}$$

where

$$\mathcal{A}(k) \triangleq \tilde{\mathcal{H}}^{\mathrm{T}} R(k) \tilde{\mathcal{H}} + \eta(k) I_{l_{\tilde{U}}},$$
$$\mathcal{B}(k) \triangleq 2\tilde{\mathcal{H}}^{\mathrm{T}} R(k)[Z(k) - \tilde{\mathcal{H}}\tilde{U}(k-1)],$$
$$\mathcal{C}(k) \triangleq Z^{\mathrm{T}}(k) R(k) Z(k) - 2Z^{\mathrm{T}}(k) R(k) \tilde{\mathcal{H}}\tilde{U}(k-1) + \tilde{U}^{\mathrm{T}}(k-1)\tilde{\mathcal{H}}^{\mathrm{T}} R(k) \tilde{\mathcal{H}}\tilde{U}(k-1).$$

If either $\tilde{\mathcal{H}}$ has full column rank or $\eta(k) > 0$, then $\mathcal{A}(k)$ is positive definite. In this case, $\bar{J}(\hat{\tilde{U}}(k-1), k)$ has the unique global minimizer

$$\hat{\tilde{U}}(k-1) = -\frac{1}{2}\mathcal{A}^{-1}(k)\mathcal{B}(k). \tag{29}$$

Next, let d be a positive integer such that $\tilde{U}(k-1)$ contains $u(k-d)$ and define the cumulative cost function

$$J_{\mathrm{R}}(\theta, k) \triangleq \sum_{i=d+1}^{k} \lambda^{k-i} \|\phi^{\mathrm{T}}(i-d-1)\theta^{\mathrm{T}}(k) - \hat{u}^{\mathrm{T}}(i-d)\|^2 + \lambda^k (\theta(k) - \theta_0) P_0^{-1} (\theta(k) - \theta_0)^{\mathrm{T}}, \tag{30}$$

where $\|\cdot\|$ is the Euclidean norm, and $\lambda \in (0, 1]$ is the forgetting factor. Minimizing (30) yields

$$\theta^{\mathrm{T}}(k) = \theta^{\mathrm{T}}(k-1) + \beta(k) P(k-1)\phi(k-d-1) \cdot [\phi^{\mathrm{T}}(k-d) P(k-1) \phi(k-d-1) + \lambda(k)]^{-1} \cdot [\phi^{\mathrm{T}}(k-d-1)\theta^{\mathrm{T}}(k-1) - \hat{u}^{\mathrm{T}}(k-d)],$$

where $\beta(k)$ is either zero or one. The error covariance is updated by

$$P(k) = \beta(k)\lambda^{-1} P(k-1) + [1 - \beta(k)] P(k-1) - \beta(k)\lambda^{-1} P(k-1)\phi(k-d-1) \cdot [\phi^{\mathrm{T}}(k-d-1) P(k-1)\phi(k-d) + \lambda]^{-1} \cdot \phi^{\mathrm{T}}(k-d-1) P(k-1).$$

We initialize the error covariance matrix as $P(0) = \alpha I_{2n_c}$, where $\alpha > 0$. Note that when $\beta(k) = 0$, $\theta(k) = \theta(k-1)$ and $P(k) = P(k-1)$. Therefore, setting $\beta(k) = 0$ switches off the controller adaptation, and thus freezes the control gains. When $\beta(k) = 1$, the controller is allowed to adapt.

B. The Phase Shift

We use the phase shift between the command input $r(k)$ and the output $y(k)$ and the command-following error $z(k)$ to investigate whether the output of the Prandtl-Ishlinskii NARMAX (PIN) controller inverts the Hammerstein system consisting of the linear plant $G(z)$ and a memoryless or hysteretic nonlinearity. To assess performance, we consider the phase shift of the most significant harmonic component in the output $v(k)$.

V. Numerical Examples

A. *Numerical Examples: Linear systems*

In this section we consider

$$x(k+1) = Ax(k) + Bu(k), \tag{31}$$
$$y(k) = Cx(k), \tag{32}$$
$$z(k) = r(k) - y(k), \tag{33}$$

which may be stable or unstable.

Example 5.1: We consider the command $r(k) = 2\sin(\omega k) + \sin(\frac{\omega}{2}k)$, where $\omega = \frac{\pi}{10}$ rad/sample with the asymptotically stable linear plant $G(z) = \frac{z-0.5}{(z-0.9)(z-0.6)}$. We use the Prandtl-Ishlinskii NARMAX (PIN) controller with $n_c = 8$ and $P_0 = 0.01$. Figure 1 shows the simulation results. ■

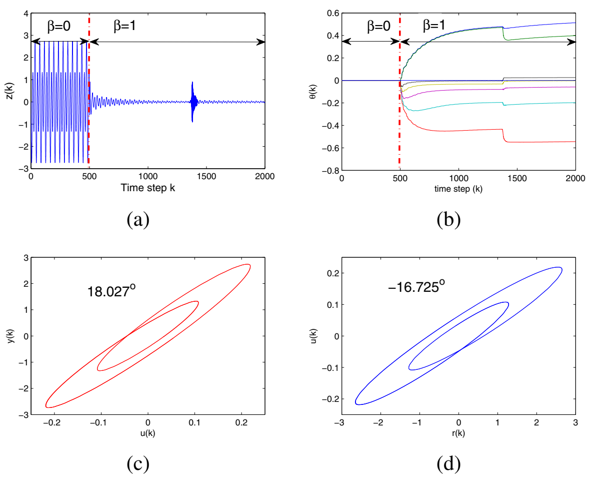

Fig. 1. Example 5.1: (a) shows the error for the command signal $r(k) = 2\sin(\omega k) + \sin(\frac{\omega}{2})$, where $\omega = \frac{\pi}{10}$ rad/sample and the asymptotically stable linear plant $G(z) = \frac{z-0.5}{(z-0.9)(z-0.6)}$. (b) shows the evolution of the controller coefficients θ, (c) shows $r(k)$ versus $u(k)$, and (d) shows $u(k)$ versus $y(k)$.

Example 5.2: We consider the command $r(k) = 2\sin(\omega k) + \sin(\frac{\omega}{2}k)$, where $\omega = \frac{\pi}{10}$ rad/sample with the Lyapunov stable plant $G(z) = \frac{1}{z-1}$. We use the Prandtl-Ishlinskii NARMAX (PIN) controller with $n_c = 8$ and $P_0 = 0.01$. Figure 2 shows the simulation results. ■

Example 5.3: We consider the command $r(k) = 2\sin(\omega k) + \sin(\frac{\omega}{2}k)$, where $\omega = \frac{\pi}{10}$ rad/sample with the unstable plant $G(z) = \frac{z-0.5}{(z-1.1)(z-0.6)}$. We use the Prandtl-Ishlinskii NARMAX (PIN) controller with $n_c = 8$ and $P_0 = 0.01$. Figure 3 shows the simulation results. ■

B. *Numerical Examples: Hammerstein systems with memoryless nonlinearities*

In this section we consider Hammerstein systems with memoryless nonlinearities.

Example 5.4: We consider the following saturation non-

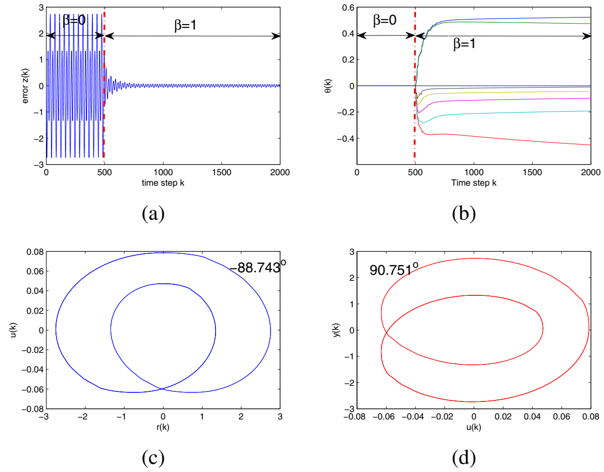

Fig. 2. Example 5.2: (a) shows the error for the command signal $r(k) = 2\sin(\omega k) + \sin(\frac{\omega}{2}k)$, where $\omega = \frac{\pi}{10}$ rad/sample and the asymptotically stable linear plant $G(z) = \frac{z-0.5}{(z-0.9)(z-0.6)}$. (b) shows the evolution of the controller coefficients θ, (c) shows $r(k)$ versus $u(k)$, and (d) shows $u(k)$ versus $y(k)$.

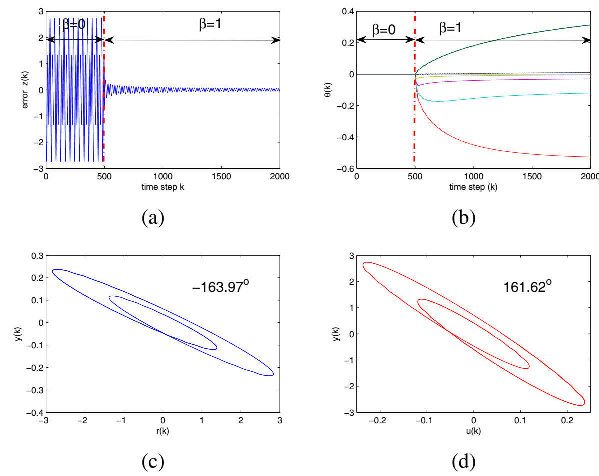

Fig. 3. Example 5.3:(a) shows the error for the command signal $r(k) = 2\sin(\omega k) + \sin(\frac{\omega}{2})$, where $\omega = \frac{\pi}{10}$ rad/sample and the unstable plant $G(z) = \frac{z-0.5}{(z-1.1)(z-0.6)}$. (b) shows the evolution of the controller coefficients θ, (c) shows $r(k)$ versus $u(k)$, and (d) shows $u(k)$ versus $y(k)$.

linearity

$$\mathcal{N}(u) = \begin{cases} \kappa, & \text{if} \quad u \geq \kappa, \\ u, & \text{if} \quad -\kappa \leq u \leq \kappa, \\ -\kappa & \text{if} \quad u \leq \kappa, \end{cases} \tag{34}$$

where $\kappa = 0.1$. We consider the command $r(k) = 3\sin(\omega k) + 2\sin(\frac{\omega}{2}k)$, $\omega = \frac{\pi}{10}$ rad/sample with the Lyapunov stable plant $G(z) = \frac{1}{z-1}$. We use the Prandtl-Ishlinskii NARMAX (PIN) controller with $n_c = 8$ and $P_0 = 0.1$. Figure 4 shows the simulation results. ■

Example 5.5: We consider the deadband nonlinearity

$$\mathcal{N}(u) = \begin{cases} u, & \text{if} \quad u \geq \sigma \quad \text{or} \quad u \leq -\sigma, \\ 0, & \text{if} \quad -\sigma \leq u \leq \sigma, \end{cases} \tag{35}$$

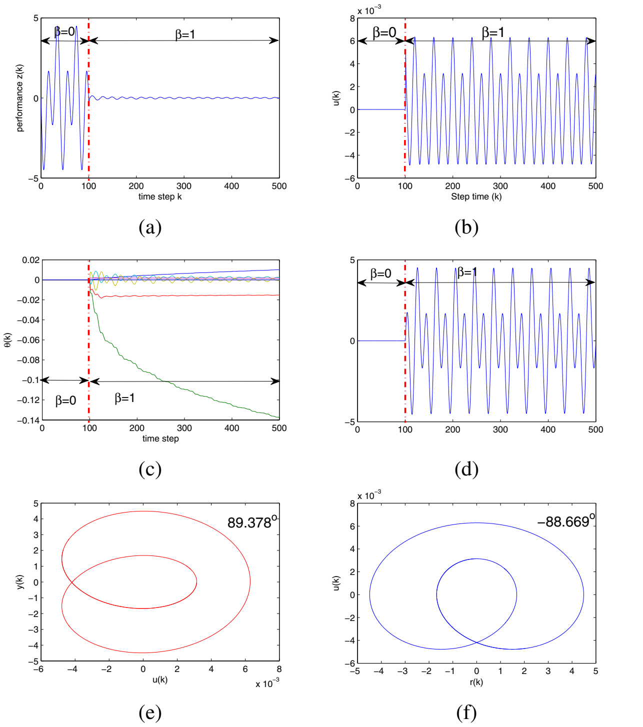

Fig. 4. Example 5.4:(a) shows the command following error z with the Lyapunov stable plant $G(z) = \frac{1}{z-1}$ and the saturation nonlinearity (34), (b) shows the control signal $u(k)$, (c) shows the evolution of the controller coefficients θ, (d) shows the output $y(k)$, (e) shows $r(k)$ versus $u(k)$, (f) shows $u(k)$ versus $y(k)$.

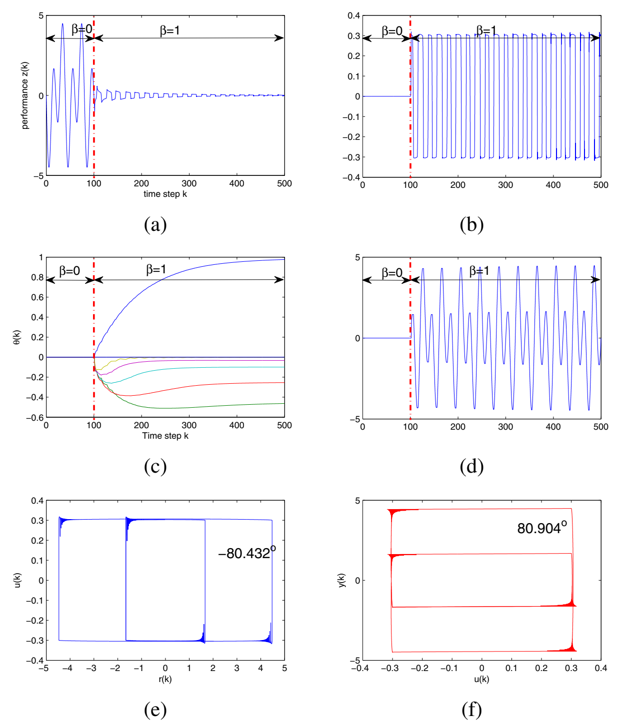

Fig. 5. Example 5.5: (a) shows the command following error z with the Lyapunov stable plant $G(z) = \frac{1}{z-1}$ and the saturation nonlinearity (34), (b) shows the control signal $u(k)$, (c) shows the evolution of the controller coefficients θ, (d) shows the output $y(k)$, (e) shows $r(k)$ versus $u(k)$, (f) shows $u(k)$ versus $y(k)$.

where $\sigma = 0.2$. We consider the command $r(k) = 3\sin(\omega k) + 2\sin(\frac{\omega}{2}k)$, $\omega = \frac{\pi}{10}$ rad/sample with the Lyapunov stable plant $G(z) = \frac{1}{z-1}$. We use the Prandtl-Ishlinskii NARMAX (PIN) controller with $n_c = 8$ and $P_0 = 0.1$. Figure 5 shows the simulation results. ■

C. Numerical Examples: Hammerstein systems with hysteretic nonlinearities

In this section we consider the Hammerstein systems with hysteretic nonlinearities.

Example 5.6: We consider the backlash nonlinearity

$$v(k) = \max\{u(k) - d_\eta, \min\{u(k) + d_\eta, v(k-1)\}\}, \quad (36)$$

with

$$v(1) = \max\{u(1) - d_\eta, \min\{u(1) + d_\eta, 0\}\}, \quad (37)$$

where $d_\eta = 0.2$. We consider the command $r(k) = 3\sin(\omega k) + 2\sin(\frac{\omega}{2}k)$, $\omega = \frac{\pi}{10}$ rad/sample with the Lyapunov stable plant $G(z) = \frac{1}{z-1}$. We use the Prandtl-Ishlinskii NARMAX (PIN) controller with $n_c = 8$ and $P_0 = 0.1$. Figure 6 shows the simulation results. ■

Example 5.7: We consider the sampled-data Duhem hysteresis model

$$\dot{v}(t) = \kappa_1|\dot{u}(t)|(\kappa_2 u(t) - v(t)) + \kappa_3\dot{u}(t), \quad (38)$$

where the positive constants $\kappa_1 = 1$, $\kappa_2 = 2$, and $\kappa_3 = 1$ determine the shape and the area of the hysteresis loop. The model (38) is implemented using Simulink with sampling

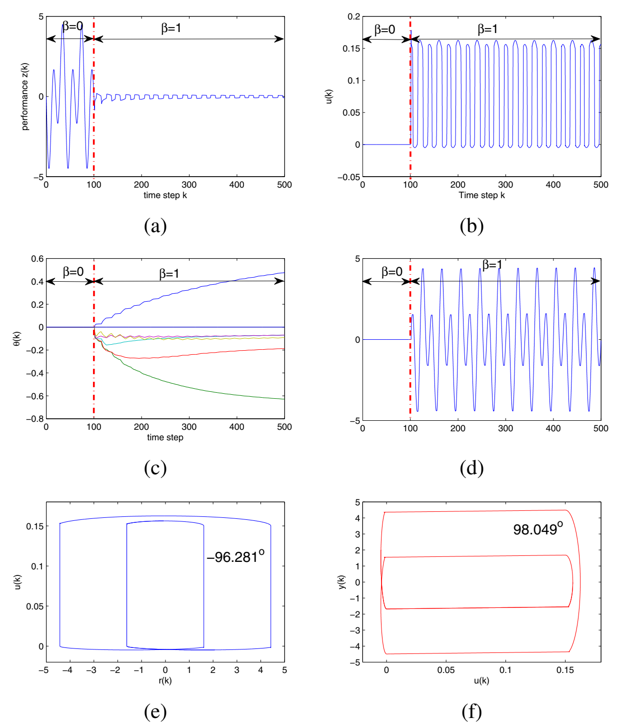

Fig. 6. Example 5.6: (a) shows the command following error z with the Lyapunov stable plant $G(z) = \frac{1}{z-1}$ and backlash nonlinearity (36), (b) shows the control signal $u(k)$, (c) shows the evolution of the controller coefficients θ, (d) shows the output $y(k)$, (e) shows $r(k)$ versus $u(k)$, (f) shows $u(k)$ versus $y(k)$.

time T_s. We consider the command $r(k) = 3\sin(\omega k) + 2\sin(\frac{\omega}{2}k) + \sin(\frac{10\omega}{6}k)$, $\omega = \frac{\pi}{10}$ rad/sample with the stable plant $G(z) = \frac{z-0.8}{(z-0.3)(z-0.6)}$. We use the adaptive Prandtl-Ishlinskii controller with $n_c = 8$ and $P_0 = 0.1$. Figure 7 shows the simulation results. ∎

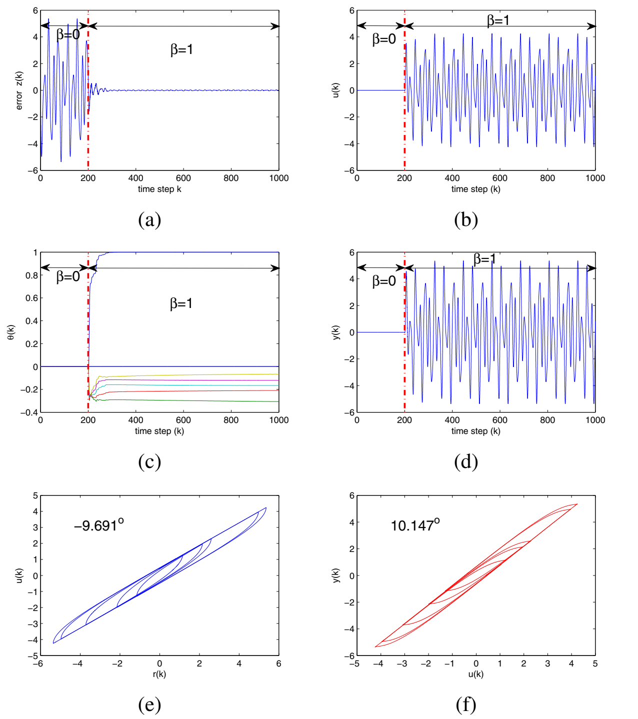

Fig. 7. Example 5.7: (a) shows the command following error z, (b) shows the control signal $u(k)$, (c) shows the evolution of the controller coefficients θ, (d) shows the output $y(k)$, (e) shows $r(k)$ versus $u(k)$, (f) shows $u(k)$ versus $y(k)$.

Example 5.8: We consider the sampled-data Bouc-Wen hysteresis model

$$\dot{v}(t) = \kappa_1 \dot{u}(t) - \kappa_2 |\dot{u}(t)||v(t)|^{n-1} v(t) - \kappa_3 \dot{u}(t)|v(t)|^n, \tag{39}$$

where the positive constants $\kappa_1 = 1$, $\kappa_2 = 2$, $\kappa_3 = 0.1$, and $n = 2$ determine the shape and the area of the hysteresis loop. The model (39) is implemented using Simulink with sampling time T_s. We consider the command $r(k) = 0.3\sin(\omega k) + 0.2\sin(\frac{\omega}{2}k) + 0.3\sin(\frac{10\omega}{6}k)$, $\omega = \frac{\pi}{10}$ rad/sample with the stable plant $G(z) = \frac{z-0.8}{(z-0.3)(z-0.6)}$. We use the Prandtl-Ishlinskii NARMAX (PIN) controller with $n_c = 8$ and $P_0 = 0.1$. Figure 8 shows the simulation results. ∎

VI. CONCLUSIONS

The numerical investigation is carried out to show that the proposed Prandtl-Ishlinskii NARMAX (PIN) control law can achieve internal model control in the presence of the plant input nonlinearities. In the future work, theoretical studies will be carried out.

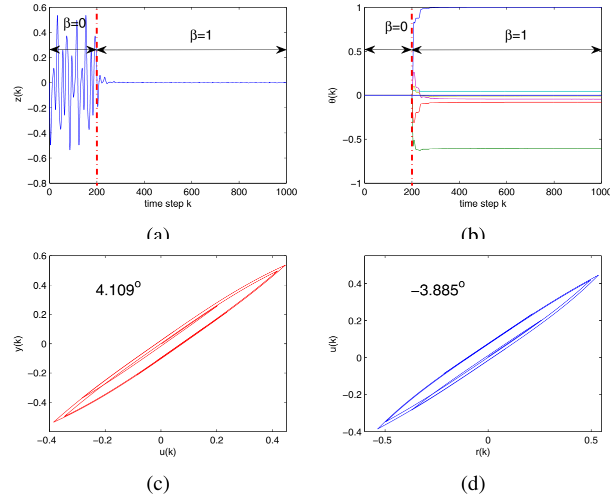

Fig. 8. Example 5.8: (a) shows the command following error z, (b) shows the control signal $u(k)$, (c) shows the evolution of the controller coefficients θ, (d) shows the output $y(k)$, (e) shows $r(k)$ versus $u(k)$, (f) shows $u(k)$ versus $y(k)$.

REFERENCES

[1] D. Angeli, J. Ferrell,and E. Sontag, "Detection of multistability, bifurcations, and hysteresis in a large class of biological positive-feedback systems," *Proc Natl Acad Sci*, vol. 101, no. 7, pp. 1822-1827, 2004.

[2] J. Kopfov, "Hysteresis in biological models," *J. Phys.: Conf. Series*, vol. 55, pp. 130-134, 2006.

[3] G. Tao and P. V. Kokotović, *Adaptive Control of Systems with Actuator and Sensor Nonlinearities*, Wiley, 1996.

[4] M. Brokate and J. Sprekels, *Hysteresis and Phase Transitions*, Springer, Berlin, 1996.

[5] D.S. Bernstein, "Ivory Ghost," *IEEE Contr. Sys. Mag.*, vol. 27, no. 5., 2007, pp. 16-17.

[6] S. Chen and S. Billings, "Representations of non-linear systems: the NARMAX model," *Int. J. Contr.*, vol. 49, no. 3, 1989, pp. 1013-1032.

[7] T. Johansen and B. Foss, "Constructing NARMAX models using ARMAX models," *Int. J. Contr.*, vol. 58, no. 5, pp. 1125-1153, 1993.

[8] J. Yan and D. S. Bernstein, "Retrospective Cost Adaptive NARMAX Control of Uncertain Hammerstein Systems Using Ersatz Nonlinearities," *AIAA Guid. Nav. Contr. Conf.*, Boston, MA, August 2013, AIAA-2013-4851.

[9] J. B. Hoagg and D. S. Bernstein, "Retrospective Cost Adaptive Control for Nonminimum-Phase Discrete-Time Systems Part 1: The Ideal Controller and Error System; Part 2: The Adaptive Controller and Stability Analysis," *Proc. Conf. Dec. Contr.*, pp. 893-904, Atlanta, GA, December 2010.

[10] M. Al Janaideh and D. S. Bernstein, "Inversion-Free Adaptive Control of Uncertain Systems with Shape-Memory-Alloy Actuation," *Proc. Amer. Contr. Conf.*, pp. 3585–3590, Washington, DC, 2013.

[11] J. Slotine and W. Li, *Applied Nonlinear Control*, Prentice-Hall, NJ, 1991.

[12] M. Al Janaideh, E. Sumer, J. Yan, A. D'Amato, B. Drincic, K. Aljanaideh, and D. Bernstein, "Adaptive Control of Uncertain Linear Systems with Uncertain Hysteretic Input Nonlinearities," In the proceedings of the 5th Annual Dynamic Systems and Control Conference, Lauderdale, Florida, USA, October 2012.

[13] M. Al Janaideh and P. Krejci, "Inverse rate-dependent PrandtlIshlinskii model for feedforward compensation of fysteresis in a piezomicropositioning actuator," *IEEE/ASME Trans. Mech.*, vol. 18, pp. 1498-1507, 2013.

[14] M. Al Janaideh and P. Krejčí, "An inversion formula for a Prandtl-Ishlinskii operator with time dependent thresholds," *Physica B*, vol. 406, no. 8, pp. 1528-1532, 2011.